# On the Continuous-time Consensus Problems with Markovian Switching

Evgeniy Grechnikov and Ricardo Vieira Godoy

***Abstract*—**In this paper, we study the linear distributed asymptotic consensus problem for a network of dynamic agents whose communication network is modeled by a randomly switching graph. A finite state Markov process dominates each topology corresponding to a state of the process. We address both the cases where the dynamics of the agents is expressed in continuous and discrete time. As long as the consensus matrices are doubly stochastic, convergence to average consensus can be shown to be achieved in the mean square and almost sure sense. A necessary and sufficient condition is the graph resulted from the union of graphs corresponding to the states of the Markov process contains a spanning tree.

***Keywords*—** Consensus problem, multi-agent systems, Markovian jump linear system, Riccati inequality, random topologies.

## I. Introduction

In the last decade, the need to exploit renewable energy resources have been provided an impetus, by many governing bodies through favorable policy making and investment. One of the renewable energy sources which has grown significantly over the last few decades and is still growing in leaps and bounds is wind energy [1], [2]. Fig.1 shows that the wind turbine capacity worldwide has grown exponentially from 1996 to 2011 with the global cumulative wind capacity reaching 250,000MW by the end of 2011 [3].

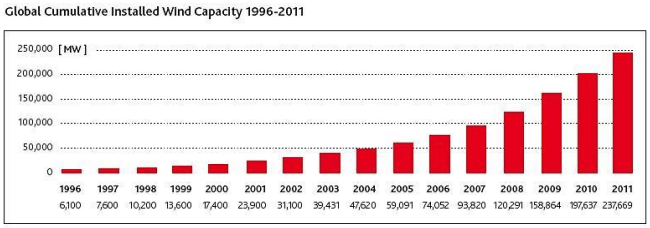


Fig.1: Development of global wind capacity from 1996 to 2011 [3].

E. Grechnikov is with Lomonosov Moscow State University, Russia (e-mail: grechnikov@gmail.com).

RV Godoy is with the University of Sao Paulo at Sao Carlos, SP, Brazil (e-mail: rvgodoy@sc.usp.br).

This rapid growth has not only been stimulated by financial support from various governments, but also from private investors. As wind turbines increase in size and power, the control mechanisms associated with them become more complex.

Control systems help drive down operating costs and improve performance. In order to achieve very accurate predictions of loading conditions, its effect on system dynamics and performance, high order mathematical models are required. Higher order models, in turn, result in controller designs being computationally intensive and oftentimes time-consuming due to numerical complexities. One of the ways to streamline controller design is to investigate methods which would facilitate model order reduction while retaining all the inherent system dynamics. A Wind Energy Conversion System (WECS) is an example of a physical system, with slow and fast dynamics arising from mechanical and electrical interactions respectively. Furthermore, there can be slow and fast subsystems within the mechanical interactions of a WECS. Such systems which evolve on different time scales are called singularly perturbed or time scale systems. The applications of singular perturbation and time scale theory spans diverse fields of engineering such as aerospace, electrical, chemical and biological systems [4], [5].

Conventional modeling methods reported in literature neglect the fast dynamics, for WECS models characterized with time scale behavior. There are numerous such instances where this approach is adopted. Rawn *et. al.* [6] consider a two mass model of a WECS and equate the fast dynamics to zero under the assumption that the faster states of the system are stable and settle to steady-state values. A similar assumption to obtain quasi steady state solutions, by neglecting the fast dynamics is seen in [7]. On the same lines [8], [9] and [10] neglect the fast states to reduce a higher order WECS model. Even though neglecting the fast dynamics facilitates ease of controller design, the solutions obtained from such a reduced order model do not satisfy all the boundary conditions of the original system. Certain systems become unstable when its fast dynamics are neglected [11].

This paper investigates the time scale method to enable model order reduction and design of a computationally inexpensive controller for WECS, by separating the original system into slow and fast subsystems. This method preserves

the system dynamics in the process. Nguyen *et. al.* in [12], [13] investigated the time scale method for WECS where the dynamics of the original system was decoupled into a 'slow' mechanical subsystem and a 'fast' electrical subsystem. Here, the mechanical interactions within a WECS are analyzed which are further separated into slow and fast subsystems depending on the moment of inertia of the turbine rotor and generator.

This paper is organized as follows: Section II presents the dynamic model of a WECS. Section III discusses the time scale method for a deterministic WECS in which the full order model is decoupled into reduced order slow and fast subsystems. Section IV deals with the design of a Linear Quadratic Regulator (LQR) for the reduced order subsystems. The LQR control is also applied to the nonlinear WECS model. In Section V, a Linear Quadratic Gaussian (LQG) control is designed for a stochastic WECS using the time scale approach. Section VI presents the simulation results for the full order and reduced order optimal control and a comparison between them is provided.

## II. WECS DYNAMICS

WECS transforms the kinetic energy of the wind into electrical energy. The wind turbine rotor serves as the transducer which harvests this wind energy. In this paper, the main focus is on the aerodynamics and the drive train dynamics of the wind energy system. This research confines itself to the time scale behavior within the mechanical interactions of the WECS. The schematic of a variable speed wind turbine is shown in Fig. 2[14].

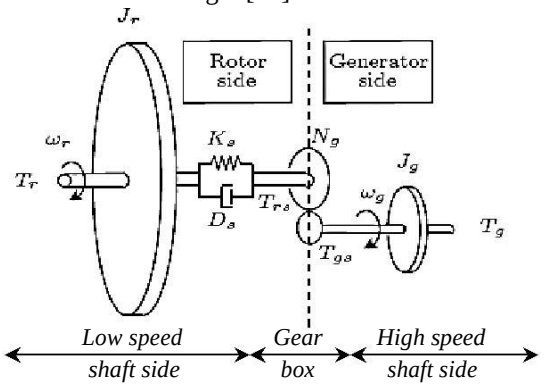

Fig.2: Schematic of the WECS [14].

The moments of inertia of the turbine rotor and generator are represented by $J_r$ and $J_g$, respectively. The two masses in the model are connected by a flexible shaft characterized by stiffness $K_S$ and damping coefficient $D_s$ [15]. The flexible shaft is considered as a torsion spring connected between the masses. An ideal gear box is assumed with a gear ratio $N_g$ that relates the speed of the turbine rotor to that of the generator.

### A. Aerodynamics

The kinetic energy of the wind stream is converted to mechanical energy by the turbine rotor blades which provide the aerodynamic torque,

$$T_r = \frac{P_r}{w_r}, \tag{1}$$

where $w_r$ is the angular velocity of the rotor and $P_r$ is the aerodynamic power given by,

$$P_r = \frac{1}{2}\rho\pi R^2 v^3 C_p(\lambda), \tag{2}$$

where $\rho$ is the air density, $R$ is the blade wing radius, $v$ is the wind speed and $C_p(\lambda)$ is the power coefficient which is a function of the tip speed ratio $\lambda$. It is defined as the ratio of the wind speed to the blade tip speed [14], [16], [17], [18],

$$\lambda = \frac{v}{Rw_r}, \tag{3}$$

where $v$ is the wind speed, $R$ is the blade wing radius and $w_r$ is the angular velocity of the rotor. The power coefficient $C_p(\lambda)$ is defined as [13],

$$C_p(\lambda) = 0.22\left(\frac{116}{\lambda_t} - 5\right)e^{-\frac{12.5}{\lambda_t}}, \tag{4}$$

$$\frac{1}{\lambda_t} = \lambda - 0.035. \tag{5}$$

### B. Drive Train Dynamics

The drive train system is approximated by a two-mass spring and damper model [7], [14], [19]. This model yields a more accurate response of the wind turbine's dynamic behavior during fluctuating wind conditions and results in a more accurate prediction of the impact on the power system [20], [21].

The mechanical model is driven by two torques, one from the turbine blades $T_r$ and the other from the electromagnetic torque $T_g$ exerted by the interacting fields of the generator. These torques cause the rotor and the generator to move with angular velocities $w_r$ and $w_g$ respectively. The equations of motion for the drive train system are obtained by summing the torques acting on each of the masses $J_r$ and $J_g$ [22].

$$\begin{aligned} \dot{w}_r &= \frac{1}{J_r}\left(\frac{P(w(t), v(t))}{w_r} - K_s\theta_{diff} - D_s\left(w_r - \frac{w_g}{N_g}\right)\right), \\ \dot{\theta}_{diff} &= w_r - \frac{w_g}{N_g}, \\ \dot{w}_g &= \frac{1}{J_g}\left(\frac{K_s\theta_{diff}}{N_g} + \frac{D_s}{N_g}\left(w_r - \frac{w_g}{N_g}\right) - T_g\right), \end{aligned} \tag{6}$$

where $\theta_{diff} = \theta_r - \theta_g$ is the difference between the angular displacements of turbine rotor and generator respectively.

### C. Non-linear Model of WECS

The nonlinear state space model of WECS is obtained by combining (1-6). Comparing the state-space model to a

nonlinear system representation $\boldsymbol{x} = f(\boldsymbol{x}, \boldsymbol{u})$, the state vector $\boldsymbol{x}$, input vector $\boldsymbol{u}$ and output vector $\boldsymbol{y}$ are defined as,

$$\begin{aligned} \boldsymbol{x} &= \begin{bmatrix} w_r & \theta_{diff} & w_g \end{bmatrix}^T, \\ \boldsymbol{u} &= \begin{bmatrix} v & T_g \end{bmatrix}^T, \\ \boldsymbol{y} &= w_g . \end{aligned} \tag{7}$$

In the WECS model, wind is a natural input to the system and since it cannot be controlled, for controller design purposes, only one control input ( $T_g$ ) is considered. Wind turbine data [14] of a Vestas-v29 225KW wind turbine was used for simulations.

### D. Eigenvalues of WECS

To understand system behavior, the nonlinear model (1- 6) was linearized about an operating point which was at the maximum power conversion efficiency. A wind speed of 11m/s was chosen for linearization. The eigenvalues obtained were: -0.090002, -7.0573 + 36.892*i* and -7.0573 - 36.892*i*. By comparing the eigenvalues, it is evident that the real eigenvalue (-0.090002) is much smaller than the real part of the complex eigenvalues (-7.0573 ± 36.892*i)*. Systems characterized by widely separated groups of eigenvalues exhibit time scale phenomena [11]. Thus the presence of one slowly varying state and two fast states can be inferred. This separation in the 'speed' of the mechanical variables makes WECS a prime candidate for Time Scale Analysis [11].

The slow dynamics in the system is attributed to the large inertia of the turbine rotor, while the fast dynamics to the relatively small inertia of the generator and poorly damped drive train dynamics. Since the nonlinear model is dependent on wind speed, linearization is carried out at various wind speeds and the eigenvalues at every wind speed indicated time scale behavior. Table 1 lists the eigenvalues corresponding to various wind speed values.

Table 1: Eigenvalues of WECS at different wind speed conditions.

| **Wind Input** | **Eigenvalues** |
|---|---|
| *v* =14 m/s | -7.0597 +36.8919i<br>-7.0597 -36.8919i<br>-0.1619 |
| *v* =16 m/s | -7.0604 +36.8918i<br>-7.0604 -36.8918i<br>-0.1832 |
| *v* =18 m/s | -7.0609 +36.8917i<br>-7.0609 -36.8917i<br>-0.1983 |
| *v* =20 m/s | -7.0613 +36.8916i<br>-7.0613 -36.8916i<br>-0.2106 |
| *v* =22 m/s | -7.0617 +36.8915i<br>-7.0617 -36.8915i<br>-0.2218 |

## III. Time Scale Analysis Of Deterministic WECS

A brief description of the time scale method [11] is provided in this section. The general form of a linear singularly perturbed system is provided in (8),

$$\begin{aligned} \dot{x}_1 &= A_{11} x_1 + A_{12} x_2 + B_{11} u, \\ \varepsilon \dot{x}_2 &= A_{21} x_1 + A_{22} x_2 + B_{21} u, \end{aligned} \tag{8}$$

where $x_1$ and $x_2$ are the *m*- and *n*- dimensional state vectors, $u$ is an *r*-dimensional control vector, matrices $A_{ij}$ and $B_{ij}$ are of appropriate dimensions and $\varepsilon$ is the small parameter representing small time constants, masses, moments of inertias, resistances, inductances or capacitances which are responsible for increasing the order of the system [11].

### A. Decomposition of System Dynamics

A two-stage linear transformation [11] , given by

$$\begin{aligned} x_s &= x_1 - M x_f , \\ x_f &= x_2 + L x_1 , \end{aligned} \tag{9}$$

is applied on the system in (8) to decouple it into independent slow and fast subsystems,

$$\begin{aligned} \dot{x}_s(t) &= A_s x_s(t) + B_s u(t), \\ \dot{x}_f(t) &= A_f x_f(t) + B_f u(t), \end{aligned} \tag{10}$$

where,

$$\begin{aligned} A_s &= A_1 - A_2 L, \\ A_f &= A_4 + L A_2 , \\ B_s &= B_1 - M L B_1 - M B_2 , \\ B_f &= B_2 + L B_1 . \end{aligned} \tag{11}$$

The subscripts 's' and '*f*' denote slow and fast states respectively. The matrices $A_1$ to $A_4$ and $B_1$ to $B_2$ are obtained from the equations in (8) as,

$$\begin{aligned} A_1 &= A_{11}, A_2 = A_{12}, B_1 = B_{11}, \\ A_3 &= \frac{A_{21}}{\varepsilon}, A_4 = \frac{A_{22}}{\varepsilon}, B_2 = \frac{B_{21}}{\varepsilon} . \end{aligned} \tag{12}$$

The variables $L(n \times m)$ and $M(m \times n)$ are solutions of the nonlinear Lyapunov-type equations,

$$\begin{aligned} L A_1 + A_3 - L A_2 L - A_4 L &= 0, \\ (A_1 - A_2 L) M - M (A_4 + L A_2) + A_2 &= 0. \end{aligned} \tag{13}$$

It is evident from (10) that the state variables $x_s$ and $x_f$ can be solved independently of each other. The *L* and *M* matrices are iteratively calculated using the high accuracy Newton method [23]. Newton's algorithm converges quadratically in the neighborhood of the sought solution, at the rate of $O(\varepsilon^{2^i})$ where $i = 1, 2 \ldots i_{max}$.

### B. Application of Time Scale Method to WECS

The nonlinear WECS model (1-6) was transformed into a linear singularly perturbed form as shown in (8). The small parameter was identified first, through a series of operations; such as scaling of differential equations and time scale transformations. The time scale method was then applied to the

WECS model, which was linearized about an operating point (as discussed in Section II-D). The small parameter identified, was the ratio of the moment of inertia of the generator to the moment of inertia of the turbine rotor [24].

A 3rd order WECS model is reduced to two separate 1st order and 2nd order models. The reduced order slow and fast subsystems obtained are:

$$\begin{bmatrix} \dot{w}_r \\ \dot{\theta}_{diff} \\ \dot{w}_g \end{bmatrix} = \underbrace{\begin{bmatrix} -0.0633 & 0 & 0 \\ 0 & -0.2861 & -0.1473 \\ 0 & 9678.8 & -3.9345 \end{bmatrix}}_{A} \begin{bmatrix} w_r \\ \theta_{diff} \\ w_g \end{bmatrix} + \underbrace{\begin{bmatrix} -0.0013 \\ 0 \\ -0.0054 \end{bmatrix}}_{B} u$$

$$\dot{x}_s = A_s \qquad A_f \qquad \dot{x}_f \qquad B_s \qquad B_f$$

To ensure that the decomposed systems retain the slow and fast dynamics, the eigenvalues of the original system and the decomposed system were compared. Table 2 lists the eigenvalues of full order and reduced order systems. The results confirm that the time scale method decouples the system dynamics perfectly (the values obtained were same to up to six decimal places).

Table 2: Comparison of full order and reduced order eigenvalues

| **Full Order** | **Eigenvalues** |
|---|---|
| $A$ | eig($A$) = -0.063321<br>-2.1103 + 37.714i<br>-2.1103 – 37.714i |
| **Reduced Order** | **Eigenvalues** |
| $A_s$ (Slow-subsystem) | eig( $A_s$ ) = -0.063321 |
| $A_f$ (Fast-subsystem) | eig( $A_f$ )= -2.1103+37.714i<br>-2.1103– 37.714i |

## IV. Optimal Control Of Deterministic WECS Using Time Scale Analysis

In general, an optimal controller provides the best possible performance with respect to a given performance index or cost function. When the performance index is quadratic, and the optimization is over an infinite horizon, the resulting optimal control law obtained by minimizing the cost function is called Linear Quadratic Regulator (LQR). Since optimal control laws guarantee infinite gain margins, minimum phase margins of 60° and stability of closed loop systems, this theory finds numerous engineering applications [25], [26], [27]. In a WECS, when the wind turbine blades are subjected to disturbances, for example, a gust of wind, it causes a perturbation to the states of the system. The objective of a LQR is to bring the perturbed states to zero. It is assumed that all the states are measurable and the control signal is unconstrained for design purposes. The performance index is chosen to minimize the error between the perturbed state and the desired state (which is zero) for an infinite time period.

Commonly, the standard LQR design for a full order WECS does not separate the slow and fast dynamics. This section discusses LQR design for a reduced order WECS. Here, control laws are implemented for the slow and fast subsystems separately.

The slow subsystem $x_s$ which was defined in (10), has a performance index,

$$J_s = \frac{1}{2}\int_0^\infty \left[ x_s^T(t) Q_s x_s(t) + u_s^T(t) R_s u_s(t) \right] dt. \qquad (14)$$

where $Q_s$ and $R_s$ are the weighting matrices for the slow subsystem. The control signal $u_s(t)$ for the slow subsystem is calculated as:

$$u_s^*(t) = -K_s x_s(t) = -R_s^{-1} B_s^T P_s x_s(t), \qquad (15)$$

where $K_s$ is the regulator gain of the slow subsystem and the solution of the slow algebraic Riccati (16),

$$P_s A_s + A_s^T P_s + Q_s - P_s B_s R_s^{-1} B_s^T P_s = 0. \qquad (16)$$

Similarly for the fast subsystem, the LQR control is calculated as,

$$u_f^*(t) = -K_f z_f(t) = -R_f^{-1} B_f^T P_f x_f(t). \qquad (17)$$

where $P_f$ is the solution of the fast algebraic Riccati equation,

$$P_f A_f + A_f^T P_f + Q_f - P_f B_f R_f^{-1} B_f^T P_f = 0. \qquad (18)$$

A block diagram describing LQR control design for the reduced order WECS is presented in Fig. 3. The feedback control is now a composite control $u^*(t)$ i.e. sum of slow control $u_s^*(t)$ and fast control $u_f^*(t)$.

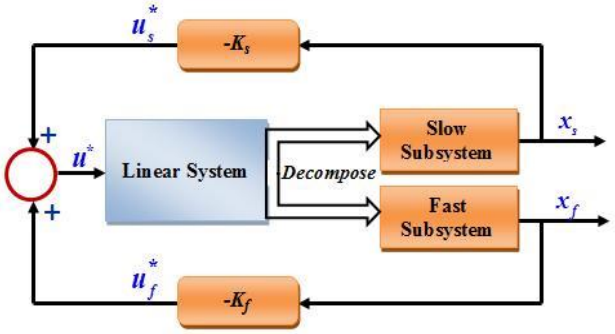


Fig.3: LQR control design for reduced order linear WECS.

The control action of the LQR was further investigated, where the composite control was studied for the original nonlinear WECS model. (Previously discussed scheme was implemented on the linear WECS model). The control scheme is depicted in Fig. 4. The states of the nonlinear WECS were simulated at nominal conditions of wind speed and control input (generator torque, $T_g$). At the point of linearization, the nominal states $x(t)$ were perturbed by a small amount $\delta x(t)$ and performance of the designed composite control was observed.

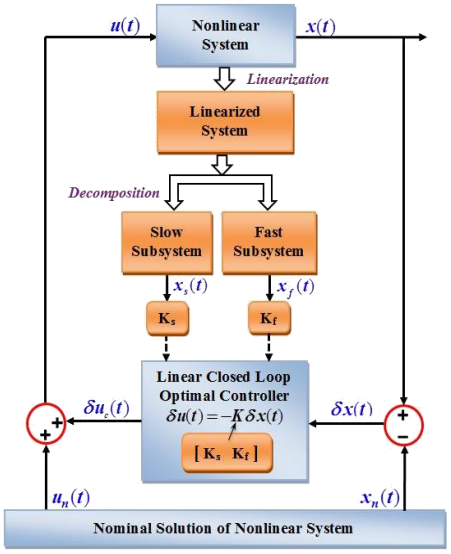


Fig.4: Reduced order LQR control design for nonlinear WECS.

## V. Optimal Control Of Stochastic WECS Using Time Scale Approach

In most cases of a variable speed wind turbine, it may not be possible to measure all the states of the system due to cost or feasibility constraints. Measurements that are available are bound to be corrupted by a certain level of noise. Also, fluctuations on the turbine blades, causes the states to be perturbed. To minimize such perturbations, a suitable controller has to be designed. In such situations, a Kalman filter is employed to get an accurate estimate of all the states of the system, which are then used to design a controller. The combined filter and regulator constitute a Linear Quadratic Gaussian (LQG) control. It is designed for controlling systems corrupted by additive white Gaussian noise, having incomplete state information and undergoing control subject to quadratic costs.

In this section, a time scale approach for solving the LQG control problem of a singularly perturbed, continuous-time, stochastic WECS system is presented. This approach is based on a closed loop decomposition technique of the optimal filters and regulators. Firstly, an optimal Kalman filter is designed for a full order stochastic WECS, followed by its time scale decomposition. Then, by utilizing the dual relationship between Kalman filters and regulators, individual slow and fast regulators are designed. These combined filters and regulators constitute the reduced order Linear Quadratic Gaussian (LQG) control.

### *A. Design of Optimal Kalman Filter for a Full-Order WECS*

Consider a linear, singularly perturbed, stochastic WECS system with a control input $u$,

$$\begin{aligned} \dot{x}_1 &= A_1 x_1 + A_2 x_2 + B_1 u + G_1 w_1 , \\ \varepsilon \dot{x}_2 &= A_3 x_1 + A_4 x_2 + B_2 u + G_2 w_1 , \\ y &= C_1 x_1 + C_2 x_2 + w_2 , \end{aligned} \tag{19}$$

and a performance index $J$ given by,

$$J = \lim_{t_f \to \infty} \frac{1}{t_f} \varepsilon \left\{ \int_0^{t_f} \left[ z^t Q z + u^t R u \right] dt \right\}, \tag{20}$$

where $z$ is the controlled output; $Q \geq 0$, $R \geq 0$ are the weighting matrices, $x_1$ and $x_2$ are the state vectors,

$$x_1 = w_r ,$$
$$x_2 = \left[ \theta_{diff} \quad w_g \right]^T ,$$

$y$ is the system measurement which measures the generator speed $w_g$ , $A_1$ to $A_4$ , $B_1$ to $B_2$ , $G_1$ to $G_2$ and $C_1$ to $C_2$ are constant matrices with appropriate dimensions, $w_1$ and $w_2$ are the system Gaussian noise and measurement Gaussian noise respectively, with intensities $W_1 \geq 0$ and $W_2 \geq 0$ respectively.

The optimal Kalman filter for the singularly perturbed WECS in (19) is obtained as:

$$\begin{aligned} \dot{\hat{x}}_1 &= A_1 \hat{x}_1 + A_2 \hat{x}_2 + B_1 u + F_1 \upsilon, \\ \varepsilon \dot{\hat{x}}_2 &= A_3 \hat{x}_1 + A_4 \hat{x}_2 + B_2 u + F_2 \upsilon, \\ \upsilon &= y - C_1 \hat{x}_1 - C_2 \hat{x}_2 , \end{aligned} \tag{21}$$

where $\hat{x}$ denotes the state estimates, $\upsilon$ is called the innovation process, $F_1$ and $F_2$ are the optimal Kalman filter gains [23],

$$\begin{aligned} F_1 &= \left( P_{1F} C_1^T + P_{2F} C_2^T \right) W_2^{-1}, \\ F_2 &= \left( \varepsilon P_{2F} C_1^T + P_{3F} C_2^T \right) W_2^{-1}. \end{aligned} \tag{22}$$

Matrices $P_{1F}$ , $P_{2F}$ and $P_{3F}$ in (22) are solutions to the filter algebraic Riccati equation (ARE),

$$A P_F + P_F A^T - P_F S P_F + G W_1 G^T = 0, \tag{23}$$

where,

$$A = \begin{bmatrix} A_1 & A_2 \\ \frac{1}{\varepsilon} A_3 & \frac{1}{\varepsilon} A_4 \end{bmatrix}, \quad P_F = \begin{bmatrix} P_{1F} & P_{2F} \\ P_{2F}^T & \frac{1}{\varepsilon} P_{3F} \end{bmatrix},$$
$$G = \begin{bmatrix} G_1 \\ \frac{1}{\varepsilon} G_2 \end{bmatrix}, \; S = C^T W^{-1} C_2 \tag{24}$$

### *B. Reduced Order LQG Control Design using Time Scale Approach*

The method for decomposing the optimal Kalman filter into independent, reduced order, slow and fast filters is presented in this section. The separate filters are such that both are driven by the system measurement instead of the innovation process $\upsilon$. Decomposition of the optimal Kalman filter is based on exact decomposition of the singularly perturbed algebraic filter Riccati equation into slow and fast Riccati equations. A transformation $\mathbf{T_2}$ is applied to the global/full order Kalman filter to obtain the decomposed slow and fast filters. Then using the duality property that exists between linear optimal filters and regulators, the LQG control is formulated [23].

The non-singular transformation $\mathbf{T_2}$ is given as:

$$\mathbf{T_2} = \left( \prod_{1F} + \prod_{2F} P_F \right), \tag{25}$$

where $P_F$ is the solution of (23), $\prod_{1F}$ and $\prod_{2F}$ matrices are

elements of the $\prod_F$ matrix,

$$\prod_F = \begin{bmatrix} \prod_{3F} & \prod_{4F} \end{bmatrix} = E_{2F}^T \begin{bmatrix} I_{2n_s} - \varepsilon NM & -\varepsilon N \\ M & I_{2n_f} \end{bmatrix} E_{1F}, \quad (26)$$

where $I_{2n_s}$ and $I_{2n_f}$ are the identity matrices of order $2n_s$ and $2n_f$. The subscripts '$n_s$' and '$n_f$' denote the number of slow and fast states in the physical system. $E_{1F}$ and $E_{2F}$ are the permutation matrices defined as :

$$E_{1F} = \begin{bmatrix} I_{n_s} & 0 & 0 & 0 \\ 0 & 0 & I_{n_s} & 0 \\ 0 & \frac{1}{\varepsilon} I_{n_f} & 0 & 0 \\ 0 & 0 & 0 & I_{n_f} \end{bmatrix}, E_{2F} = \begin{bmatrix} I_{n_s} & 0 & 0 & 0 \\ 0 & 0 & I_{n_s} & 0 \\ 0 & I_{n_f} & 0 & 0 \\ 0 & 0 & 0 & I_{n_f} \end{bmatrix}, \quad (27)$$

and $M$ & $N$ are the solutions of the Chang's decoupling equations:

$$\begin{aligned} T_{4F} M - T_{3F} - \varepsilon M (T_{1F} - T_{2F} M) = 0, \\ T_{2F} - N (T_{4F} + \varepsilon M T_{2F}) + \varepsilon (T_{1F} - T_{2F} M) N = 0. \end{aligned} \quad (28)$$

The matrices $T_{1F}$ to $T_{4F}$ are defined as:

$$\begin{aligned} T_{1F} &= \begin{bmatrix} A_1^T & -C_1^T W_1 C_2 \\ -G_1 W_1 G_1 & -A_1 \end{bmatrix}, \quad T_{2F} = \begin{bmatrix} A_3^T & -C_2^T W_2 C_1 \\ -G_1 W_1 G_2 & -A_2 \end{bmatrix}, \\ T_{3F} &= \begin{bmatrix} A_2^T & -C_1^T W_2 C_2 \\ -G_2 W_2 G_1 & -A_3 \end{bmatrix}, \quad T_{4F} = \begin{bmatrix} A_4^T & -C_2^T W_2 C_2 \\ -G_2 W_1 G_2 & -A_4 \end{bmatrix}. \end{aligned} \quad (29)$$

On applying transformation $\mathbf{T_2}$ to the filter's state variables,

$$\begin{bmatrix} \hat{\eta}_s \\ \hat{\eta}_f \end{bmatrix} = \mathbf{T}_2^{-T} \begin{bmatrix} \hat{x}_1 \\ \hat{x}_2 \end{bmatrix}, \quad (30)$$

the two independent, slow and fast Kalman filters are obtained as,

$$\begin{aligned} \dot{\hat{\eta}}_s &= (a_{1F} + a_{2F} P_{sF})^T \hat{\eta}_s + B_s u + F_s y, \\ \varepsilon \dot{\hat{\eta}}_f &= (b_{1F} + b_{2F} P_{fF})^T \hat{\eta}_f + B_f u + F_f y, \end{aligned} \quad (31)$$

where $\hat{\eta}_s$ and $\hat{\eta}_f$ are the slow and fast state estimates; $P_{sF}$ and $P_{fF}$ are the solutions of the slow and fast algebraic Riccati equations,

$$\begin{aligned} P_{sF} a_{1F} - a_{4F} P_{sF} - a_{3F} + P_{sF} a_{2F} P_{sF} = 0, \\ P_{fF} b_{1F} - b_{4F} P_{fF} - b_{3F} + P_{fF} b_{2F} P_{fF} = 0. \end{aligned} \quad (32)$$

The algebraic Riccati equations are solved by Newton's algorithm which is provided in the reference [23]. The other matrices in (32) are,

$$\begin{aligned} \begin{bmatrix} a_{1F} & a_{2F} \\ a_{3F} & a_{4F} \end{bmatrix} &= (T_{1F} - T_{2F} M), \\ \begin{bmatrix} b_{1F} & b_{2F} \\ b_{3F} & b_{4F} \end{bmatrix} &= (T_{4F} + \varepsilon M T_{2F}), \\ \begin{bmatrix} F_s \\ \frac{1}{\varepsilon} F_f \end{bmatrix} &= \mathbf{T}_2^{-T} \begin{bmatrix} F_1 \\ \frac{1}{\varepsilon} F_2 \end{bmatrix}, \end{aligned} \quad (33)$$

$$\begin{bmatrix} B_s \\ \frac{1}{\varepsilon} B_f \end{bmatrix} = \mathbf{T}_2^{-T} \begin{bmatrix} B_1 \\ \frac{1}{\varepsilon} B_2 \end{bmatrix}. \quad (34)$$

The optimal control in terms of the slow and fast Kalman filters is given by:

$$u^* = -\begin{bmatrix} K_s & K_f \end{bmatrix} \begin{bmatrix} \hat{\eta}_s \\ \hat{\eta}_f \end{bmatrix}, \quad (35)$$

where the slow and fast regulator gains $K_s$ and $K_f$ are defined as:

$$\begin{bmatrix} K_s & K_f \end{bmatrix} = (R^{-1} B^T P) \mathbf{T}_2^T, \quad (36)$$

where $P$ is the solution of the algebraic Riccati equation

$$PA + A^T P + Q - PSP = 0. \quad (37)$$

A block diagram is shown in Fig. 5 which summarizes the LQG control with reduced order Kalman filter and regulator. The control signal fed back to the WECS system is a composite control signal or sum of slow and fast control.

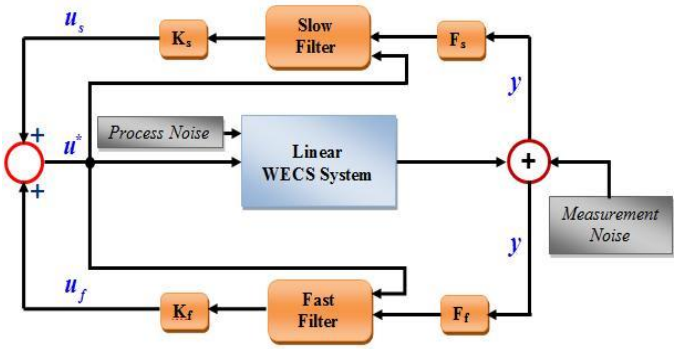


Fig.5: LQG control design of WECS with reduced order filter and regulator.

## VI. Simulation Results

All the controllers were designed in MATLAB® and implemented in Simulink®.

### A. Results of LQR Control for Deterministic WECS

The matrices $A_s$, $B_s$, $A_f$ and $B_f$ for LQR control design are given in Section III-B. The weighting matrices $Q_s$, $R_s$, $Q_f$ and $R_f$ were chosen such that they minimize the time taken by the states to attain their nominal values. These matrices were chosen from multiple iterations. A comparison between the full order and reduced order control of the linear WECS is provided in Fig. 6. It can be seen that the controller regulates all the states to zero, for both full order and reduced order cases. A detailed view of the states near the origin is shown in Fig. 7. The very close matching between the full order and reduced order LQR control manifests the effectiveness of the time scale method. Thus the proposed method provides almost the very same control action with less computational effort.

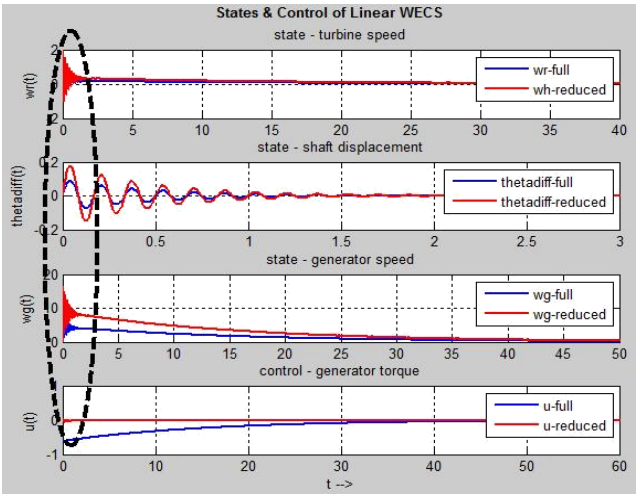


Fig.6: LQR control – Comparison of the full order system and reduced order WECS.

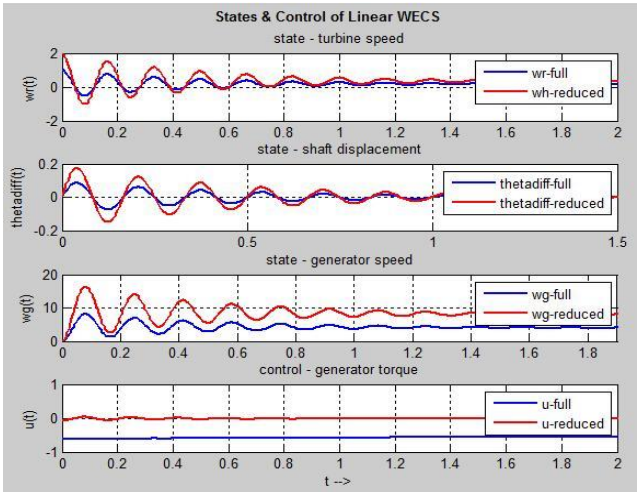


Fig.7: Detailed view of the LQR comparison plots near the origin.

The simulation results for LQR (with composite control) feedback to nonlinear WECS are provided in Fig. 8. The nominal solutions of the states are obtained by simulating the nonlinear model for wind speed of 11 m/s and generator torque of 2132 N-m. A pulse was applied to the wind speed input to perturb the nominal states of the system. The results indicate that the composite control action regulates the states of the nonlinear system to their corresponding nominal values. Fig. 8 shows that the system was perturbed at the 10 second mark, and the proposed controller brings the states back to the nominal values quickly. The dynamics of the state $\theta_{diff}$ $(t)$ (shaft displacement) indicates oscillations on application of the pulse, before the state was returned to its nominal value.

For the generator speed state $w_g$ $(t)$ , the time taken to bring the system back to the nominal values is comparatively longer. This delay can be overcome by modifying the weighting matrices $Q$ and $R$ .

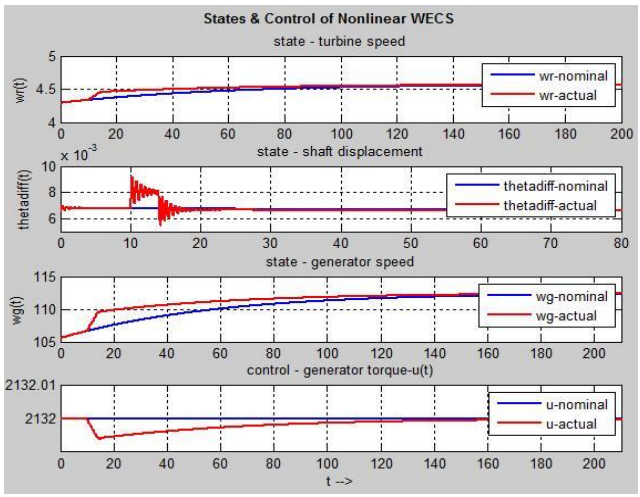


Fig.8: States and control of nonlinear WECS with composite LQR control.

*B. Results of LQG Control for Stochastic WECS*

The weighting matrices $Q$ and $R$ for the stochastic system were chosen in a similar way as for the deterministic case (Section VI-A). The process and measurement noise are assumed to be independent Gaussian noise with zero mean. The process noise, which is applied to the system states, could be on account of wind fluctuations on the turbine blades. While, measurement noise applied to the output state (generator speed) could be due to sudden changes in generator load conditions or high harmonic currents resulting from power electronics converters [28], [29]. For the simulations, the noise sources were chosen as 'Random Number' blocks from the Simulink® library. In order to see the effects of Kalman filter, in the WECS system, the states corrupted with noise are compared to their corresponding Kalman estimates. The output signal is also compared to its estimate. The results are plotted in Fig. 9. It is seen that the Kalman filtering reduces the influence of noise on the system states and output and provides good estimation.

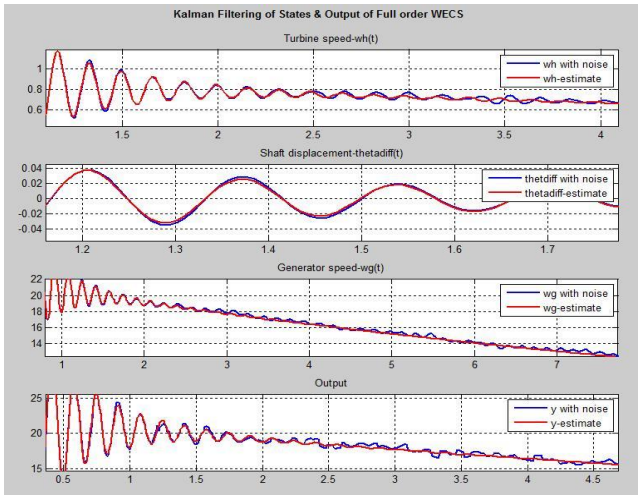


Fig.9: States and output compared to their Kalman estimates.

A comparison of the results between the full order and reduced order LQG control is provided in Fig. 10. It is observed that LQG control regulates the states of the system to zero for both full order and reduced order controllers. A detailed view of the results near the origin is provided in Fig.11.

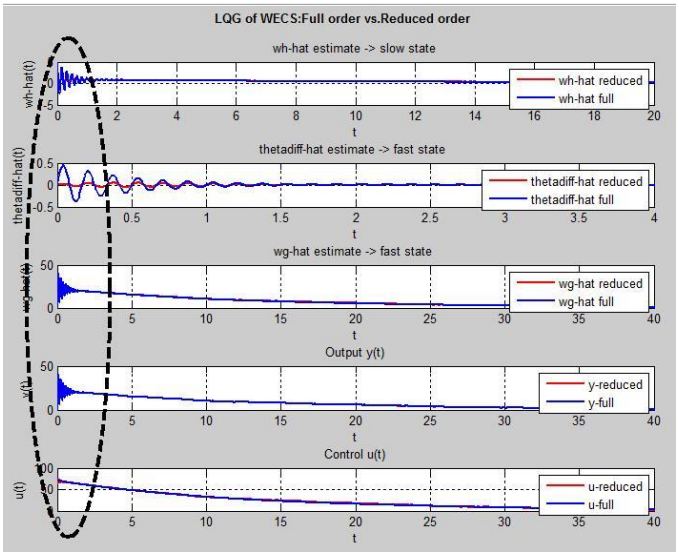


Fig.10: Comparison of full order and reduced order LQG control.

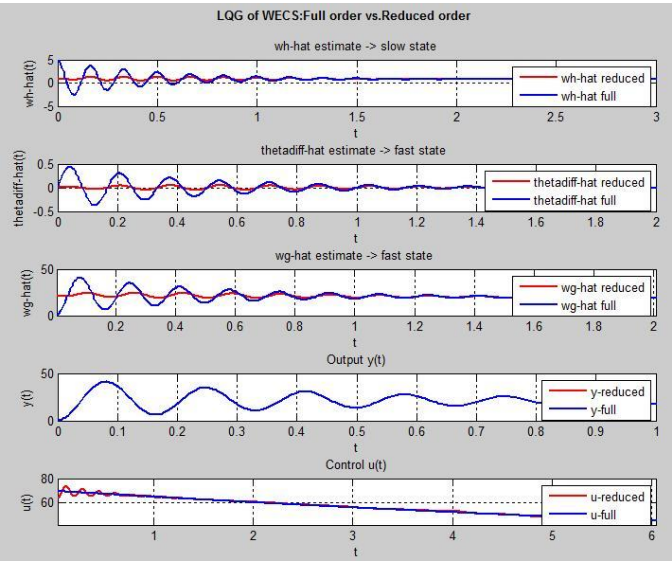


Fig.11: Detailed view of LQG comparison plots.

The closeness of the full order and the reduced order results indicate that comparable control can be achieved with the reduced order filters and regulators. The detailed view in Fig. 11 also shows that amplitudes of oscillation of the state estimates have been reduced by the implementation of the time scale design.

## VII. Discussion

A time scale analysis of the mechanical interactions of WECS was performed in this research. The prime objective was to develop a computationally less intensive controller

scheme, which was brought about by the application of the time scales method to a higher order wind energy system. The method helped bring a 3rd order WECS system and Kalman filter down to a 1st order and a 2nd order subsystem facilitating simpler optimal control designs. The simulation results for both deterministic and stochastic WECS, of a full order and a reduced order system, indicates that the performances match closely to that of the full order system. The reduced order LQR control was applied to a nonlinear WECS. From the simulation results it is evident that the proposed method does provide a comparable control even with the system perturbed.

These results shed light on the effectiveness of the proposed methodology.

## VIII. Conclusion

A time scale technique of the deterministic and stochastic WECS was proposed which led to decoupling of a full order system into independent slow and fast subsystems. The simulation results indicate that the performances of the full order system closely match that of the reduced order system. This shows that the strengths of this design approach can be exploited without loss of system dynamics. The time scale approach has important implications, especially when large model orders are used to describe a complete wind energy system (mechanical and electrical components). For real time applications, the decoupling of the full order system would bring about a reduction in on-line and off-line computational requirements. Also, the slow and fast controllers work in parallel and process information independently with their corresponding sampling rates (slow with slow sampling rate, fast with fast sampling rate). Moreover, a wind energy system designed with two controllers, for each of the slow and fast subsystems, is more reliable than a system with one controller in the event of a controller malfunction.

## References


[1] P. Musgrove, *Wind Power*, Cambridge, UK: Cambridge University Press, 2010.

[2] W. Shepherd and L. Zhang, *Electricity Generation Using Wind Power*, Singapore: World Scientific Publishing Co. Ltd, 2011.

[3] "Global Wind Report Annual Market Update," Global Wind Energy Council (GWEC), 2011.

[4] D. S. Naidu and A. J. Calise, "Singular perturbations & Time Scales in Guidance and Control of Aerospace Systems: A survey," *Journal of Guidance, Control and Dynamics*, vol. 24, no. 6, pp. 1057-1078, 2001.

[5] D. S. Naidu, "Singular perturbations and time scales in control theory and applications: An Overview," *Dynamics of Continuous, Discrete and Impulsive Systems Series*, vol. 9, no. Series B, pp. 233-278, 2002.

[6] B. G. Rawn, "Control Methodology to Mitigate the Grid Impact of Wind Turbines," *IEEE Transactions On Energy Conversion*, vol. 22, no. 2, pp. 431-438, 2007.

[7] R. O. B. Zarouala, C. Vivas, J. Á. Acosta and L. E. Bakkali, "On Singular Perturbations of Flexible and Variable-Speed Wind Turbines," *International Journal of Aerospace Engineering*, vol. 2012, 2012.

[8] D. Fu and Y. Xing, "Study of Linear Dynamic Model and analysis of Operating Characteristics of High Power VSCF Wind Energy Conversion System," in *World Non-Grid-Connected Wind Power and Energy Conference*, September 2009.